Environ Earth Sci (2012) 66:1043–1057
DOI 10.1007/s12665-011-1310-7

ORIGINAL ARTICLE

The behavior of arsenic and antimony at Pezinok mining site, southwestern part of the Slovak Republic

Renata Flakova · Zlatica Zenisova · Ondra Sracek · David Krcmar · Ivana Ondrejkova · Martin Chovan · Bronislava Lalinská · Miriam Fendekova

Received: 7 February 2011 / Accepted: 8 August 2011 / Published online: 21 August 2011

Abstract Arsenic and antimony contamination is found at the Pezinok mining site in the southwest of the Slovak Republic. Investigation of this site included sampling and analysis of water, mineralogical analyses, sequential extraction, in addition to flow and geochemical modeling. The highest dissolved arsenic concentrations correspond to mine tailings (up to 90,000 μg/L) and the arsenic is present predominately as As(V). The primary source of the arsenic is the dissolution of arsenopyrite. Concentration of antimony reaches 7,500 μg/L and its primary source is the dissolution of stibnite. Pore water in mine tailings is well-buffered by the dissolution of carbonates (pH values between 6.6 and 7.0) and arsenopyrite grains are surrounded by reaction rims composed of ferric iron minerals. Based on sequential extraction results, most solid phase arsenic is in the reducible fraction (i.e. ferric oxyhydroxides), sulfidic fraction, and residual fraction. Distribution of antimony in the solid phase is similar, but contents are lower. The principal attenuation mechanism for As(V) is adsorption to ferric oxide and hydroxides, but the adsorption seems to be limited by the competition with Sb(V) produced by the oxidation of stibnite for adsorption sites. Water in mine tailings is at equilibrium with gypsum and calcite, but far from equilibrium with any arsenic and antimony minerals. The concentrations of arsenic and antimony in the surrounding aquifer are much lower, with maximum values of 215 and 426 μg/L, respectively. Arsenic and antimony are transported by ground water flow towards the Blatina Creek, but their loading from ground water to the creek is much lower compared with the input from the mine adits. In the Blatina Creek, arsenic and antimony are attenuated by dilution and by adsorption on ferric iron minerals in stream sediments with resulting respective concentrations of 93 and 45 μg/L at the site boundary south of mine tailing ponds.

Keywords Arsenic · Antimony · Slovakia · Pezinok · Mine tailings · Attenuation

R. Flakova (✉) · Z. Zenisova · D. Krcmar · I. Ondrejkova · M. Fendekova
Department of Hydrogeology, Faculty of Natural Sciences, Comenius University, Mlynska dolina, 842 15 Bratislava, Slovak Republic
e-mail: rflakova@fns.uniba.sk

O. Sracek
Department of Geology, Faculty of Science, Palacký University, 17. listopadu 12, 771 46 Olomouc, Czech Republic

O. Sracek
OPV s.r.o. (Protection of Groundwater Ltd.), Bělohorská 31, 169 00 Praha 6, Czech Republic

M. Chovan · B. Lalinská
Department of Mineralogy and Petrology, Faculty of Natural Sciences, Comenius University, Mlynska dolina, 842 15 Bratislava, Slovak Republic

Introduction

Natural arsenic enrichment of ground water has been found at several sites around the world (Smedley and Kinniburgh 2002). In many areas, high arsenic concentration in ground water occurs naturally as a consequence of the reductive dissolution of ferric oxide and hydroxides (for example, in Bangladesh and West Bengal, India; Nickson et al. 2000; Ahmed et al. 2004), the dissolution of volcanic glass and high mobility of arsenic under high pH conditions (at the Pampean region of Argentina; Smedley et al. 2005; Bhattacharya et al. 2006) or recent geothermal activity in the Chilean Andes (Romero et al. 2003).

However, arsenic is also released as a result of mining activities (Nordstrom 2002; Smedley and Kinniburgh 2002). Arsenic in mining wastes is generally present in sulfidic minerals like arsenopyrite (FeAsS), orpiment (As_2S_3), and realgar (AsS). Dissolution of sulfidic minerals produces the highest reported concentrations of dissolved arsenic. There is arsenic contamination from arsenopyrite residue stockpile at Snow Lake, Manitoba, Canada (Salzsauler et al. 2005), where arsenic sulfides are oxidized and secondary minerals like scorodite, jarosite and Fe-sulfoarsenates precipitate. These secondary minerals are later dissolved and ground water monitoring wells adjacent to the stockpile have recorded >20 mg/L of arsenic. At the Kaňk site, close to Kutna Hora in the Czech Republic, the controlled flooding of a mine resulted in the reductive dissolution of ferric minerals formed during the dissolution of arsenopyrite and arsenic concentrations in the mine shaft water reached 59 mg/L (Kopřiva et al. 2005). Extremely high arsenic concentrations were reported from the Richmond Mine, in California (USA), where acid mine drainage (AMD) water is concentrated due to a high evaporation rate. Dissolved arsenic concentrations as high as 850 mg/L have been reported (Nordstrom and Alpers 1999). However, the highest reported dissolved arsenic concentrations found in the literature are from the Berikul gold mine in Siberia, Russia (Giere et al. 2003), where the concentrations of arsenic and sulfate in pore water of a high-sulfide pile reached 22,000 and 190,000 mg/L, respectively. The Carnoulès site, in southern France has been studied by Casiot et al. (2005). There, a low pH (<3.0) and arsenic concentrations up to 250 mg/L in mine tailings have been reported. At this site, arsenic present mostly as As(III) is attenuated by co-precipitation with schwertmannite in a creek draining the site, and further downgradient where pH becomes neutral, with Fe(III)-oxyhydroxides. Arsenic is re-mobilized during low flow periods as a consequence of desorption.

Data from several mining sites around the world have been compiled by Williams (2001). This author concludes that arsenopyrite is the main source of arsenic while the formation of poorly soluble scorodite ($FeAsO_4 \cdot 2H_2O$) limits the mobility of arsenic in ground waters. The impact of scorodite precipitation on arsenic mobility in mine tailings has been studied by Langmuir et al. (1999, 2006). They concluded that amorphous and poorly crystalline scorodite precipitates below pH 3.0 and is the dominant form of arsenate in slake-limed tailings.

There are some examples of arsenic contamination in AMD waters neutralized by the dissolution of carbonates. In the Zimapan Valley (Hidalgo state, Mexico) arsenic is released from mine tailings under high pH conditions (Armienta et al. 1993; Romero et al. 2004; Armienta and Segovia 2008; Sracek et al. 2010) and contaminates wells around the mine tailings. Uranium mine tailings at Rabbit Lake (Saskatchewan, Canada), with high arsenic concentrations and pore water pH values above 9.3 were studied by Donahue and Hendry (2003). They found that the arsenic was associated with amorphous Fe(III) oxide and hydroxides at shallow depths but, in the deep zone of the mine tailings the control of dissolved arsenic appear to be connected with a Ca-arsenate phase whose composition would be $Ca_4(OH)_2(AsO_4)_2 \cdot 4H_2O$. The formation and role of Ca-arsenate minerals has been discussed by Juillot et al. (1999) and Morin and Calas (2006). When acid water with high dissolved As concentration encounters limestone, As-minerals like weilite ($Ca(AsO_3OH)$) and pharmacolite ($CaHAsO_4 \cdot 2H_2O$) may precipitate. Oxidation of sulfides coupled to the release of arsenic may also occur under natural conditions (Schreiber et al. 2000) but, in these situations, the concentration of dissolved arsenic is generally much smaller compared to typical mining sites.

Compared to arsenic, much less is known about the behavior of antimony (Wilson et al. 2010). Antimony is produced by the oxidation of sulfidic minerals such as stibnite. Stibnite dissolves readily in oxidized water and concentrations of dissolved antimony up to 55,000 µg/L were found at Hillgrove mining site, southeastern Australia, by Ashley et al. (2003). In water, antimony occurs in oxidation states Sb(III) and Sb(V) (Filella et al. 2002). However, Sb(III) can also be present in oxidizing environments due to oxidation kinetic constraints. Under oxidizing conditions and close to neutral pH Sb(V) is present as oxyanion $Sb(OH)_6^-$ (Vink 1996) and, thus, its adsorption decreases with increasing pH (Krupka and Serne 2002), just like in the case of As(V). Similar adsorption behavior of both elements indicates their competition for adsorption sites.

Pezinok is an old mining site located in the Male Karpaty Mountains, in southwestern Slovak Republic (Fig. 1). Several sources of arsenic contamination might be found there. They include drainage from mine adits and mine tailings. The particular geology of the site, with abundant carbonates in the rock matrix determines that the pH values of mine drainage remain nearly neutral.

The objectives of this paper are: (1) to identify the processes controlling the mobility of arsenic and antimony in mine tailings and in the surrounding aquifer at Pezinok mining site and (2) to evaluate the arsenic and antimony input into the Blatina Creek, which drains the Pezinok site. Several methods were used, including sampling of water, mineralogical analyses, and geochemical and ground water modeling.

Geology and history of mining at the Pezinok mining site

The Male Karpaty Mountains is the westernmost mountain range of the Western Carpathians, linking the Carpathians

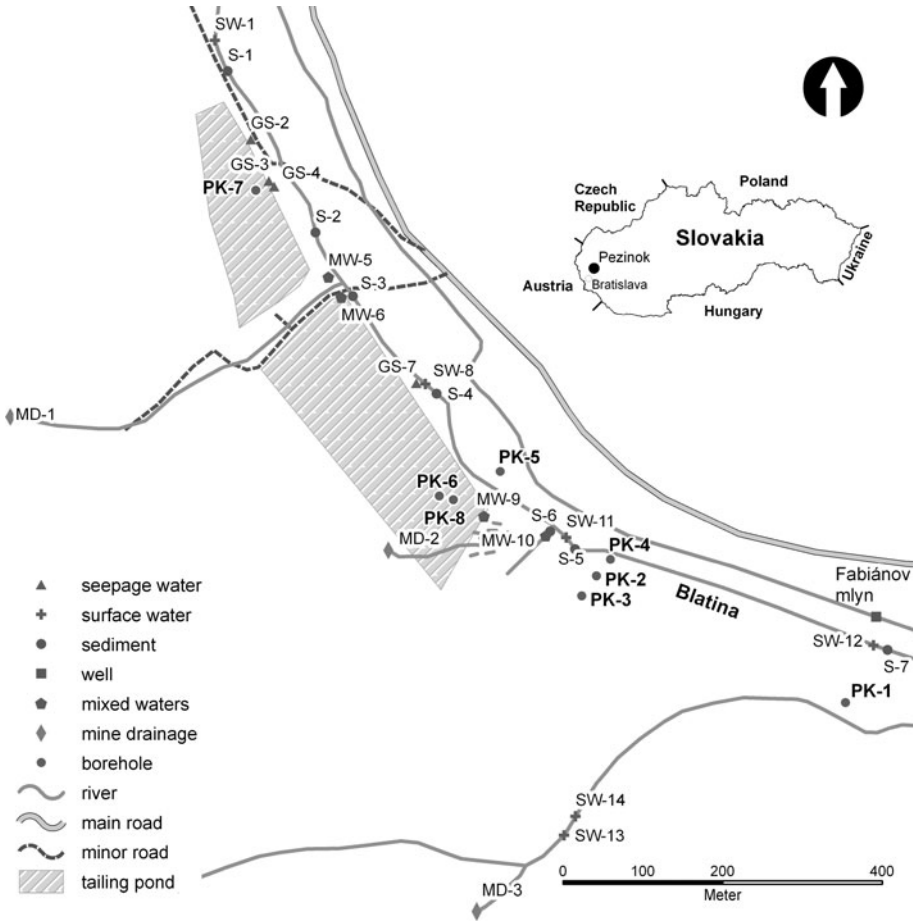

Fig. 1 Location of the Pezinok site and location of the sampling points

with the Alps. The geological structure of the Malé Karpaty Mountains is characterized by several superposed nappes, consisting of a prealpine basement, Mesozoic cover, and higher nappes. Metamorphosed, pyrite-pyrrhotite stratiform as well as later strata-bound Sb-As-Au mineralizations are the most important ore types in the Early Paleozoic rocks. These rocks, originating in the Devonian age consisting of a volcanic-sedimentary formation, have been subjected to regional and contact metamorphism in connection with intrusions of Variscan granitoids. Pyrite (FeS_2), pyrrhotite ($Fe_{(1-x)}S$) and stibnite (Sb_2S_3) mineralization occur in the form of lenses, quartz-carbonate veinlets and impregnations in black shales embedded in amphibolites, in addition to chlorite and sericite schists and amphibolites (Chovan et al. 1992). Crystalline schists are intersected by dykes of Variscan (348 Ma) granitoids.

Major ore minerals at the Pezinok–Kolársky vrch deposit include stibnite, pyrite, arsenopyrite, FeAsS, berthierite ($FeSb_2S_4$) and kermesite (Sb_2S_2O). Among the minor minerals worth mentioning are gudmundite (FeSbS), pyrrhotite, native antimony, loellingite ($FeAs_2$) and marcasite (FeS_2). The most frequent gangue minerals are quartz and carbonates (Chovan et al. 1994). In the process of hydrothermal alteration of carbonates, illite and chlorites were formed (Moravanský and Lipka 2004).

The primary ores were extracted via flotation processes. The resulting antimony concentrate was mainly composed of stibnite, berthierite, and organic matter. The rest of metallic minerals (pyrite, arsenopyrite, gudmundite, loellingite, Sb), Fe oxy-hydroxides as well as gangue minerals (quartz, carbonates, chlorites, low amounts of feldspars, amphiboles, and clay minerals, especially illite) constitute the principal waste of processing and they were deposited in mine tailings ponds.

The Quaternary deposits, which are affected by As-Sb contamination, are fluvial sediments deposited by the Blatina Creek, which flows at the eastern boundary of mine tailing ponds area (Fig. 1). The average thickness of the Quaternary sediments at the study site is about 6 m. The upper zone is composed of clayey sediments, which form the low permeability top of the sandy gravels located beneath. The average width of the Quaternary sediments in contact with mine tailings ponds along the Blatina Creek is about 150 m. Neogene clay sediments create an impervious boundary of the Quaternary aquifer.

There are two types of ores subjected to the exploitation in the Male Karpaty Mountains. The first type is the pyrite-

pyrrhotite mineralization, whose exploitation dates back to the late eighteenth century. The second type is the hydrothermal Sb-As-Au mineralization. Two Sb deposits bound to this mineralization were exploited: the Pernek deposit (1790–1922) where several abandoned waste rock piles remain, and the Kolársky Vrch deposit (1790–1992), where most intensive mining activity occurred since 1940 (Cambel 1959). The waste is deposited in two mine tailings ponds (Fig. 1). The mine water from abandoned galleries and adits, flowing out directly into surface water bodies, represents the primary source of surface water contamination in the surroundings of the Pezinok mine site. Important sources of contamination are also mine tailing ponds, which are not hydraulically isolated from the underlying layers. Mine water has brought high concentrations of sulfate, iron, aluminum, arsenic, and antimony into the surrounding environment.

Materials and methods

Drilling occurred in April 2004: eight boreholes were drilled with total length of 102 m (average borehole depth 13 m). All the drilled boreholes were equipped with PVC casing.

Field parameters monitored included temperature, pH, redox potential, and electrical conductivity. The pH was measured using a WTW Multi 350i using a electrode Sentix 41; the redox potential was measured using a WTW pH-meter 340i using a combined platinum electrode SenTix^{R}ORP equipped with a calomel reference electrode and the electrical conductivity was measured with a WTW Multi 350i using a electrode TetraCon^{R}325. Redox measurements were corrected to the standard hydrogen electrode (SHE).

Sampling points (Fig. 1) included the outlet of three different mining adits (Pyritova MD-1, Buducnost MD-2, Sirkova MD-3), four profiles of the Blatina Creek (SW-1, SW-8, SW-11, SW-12), two profiles of the Sirkovy Creek (SW-13, SW-14) and ground water discharges located at the base of the mine tailing elevation (GS-2, GS-3, GS-4, GS-7). In addition, water has also been monitored at four other locations (MW-5, MW-6, MW-9, MW-10), where it is not possible to determine whether the water is ground or surface water (there are boggy spots where ground water seepage mixes with surface drainage), and therefore, it is described as a mixture of both types (Flakova et al. 2005). Complementary measurements were taken from a domestic well belonging to a residence called Fabianov mlyn (Fig. 1).

Water samples were taken from the monitoring sites in April and November 2004. Ground water samples from boreholes were taken after renewing the well volume several times. The samples selected for the determination of trace elements (Fe, Mn, Al, Co, Cu, Ni, Zn) were filtered through a 0.45-μm filter and preserved by ultrapure HNO_3. For determination of As and Sb, the samples were filtered through a 0.45-μm filter and then preserved with ultrapure HCl. All samples were kept at 4°C until analyses. As, Sb, Se were determined by AAS (hydride generation; Spectr AA 220 fy Varian) while and Na, K, Ca, Mg, Si, Fe, Mn, Al, Cr, Cu, Zn, Co, Ni were analyzed by AES-ICP (VISTA-MPX fy Varian) at the Hydrogeochemical Laboratory of the Department of Hydrogeology, Comenius University, and in the Geoanalytical Laboratory of the Slovak Geological Survey.

Acidity was determined by titration with 0.05 M NaOH with phenolphthalein indicator, alkalinity by titration with 0.1 M HCl and methyl-orange indicator. Sulfate was determined by gravimetry after precipitation with $BaCl_2$ and Cl^- by titration with $Hg(NO_3)_2$. Concentrations of NH_4^+, NO_3^-, and HPO_4^{3-} were determined by spectrophotometry using a PERKIN ELMER UV/VIS Lambda 11 apparatus.

The measured concentrations of trace elements in the certified and synthetic standards were within 10% of their true values. Replicate analyses were carried out on selected samples and variations were in the range ±10%. A Varian spectrometer AA 220 with flame heated silica atomizing tube and automatic hydride generator was used for the determination of As. The hydride of As was generated from 3 M HCl after preliminary reduction As(V) to As(III) with 20% KI. The concentration of As(III) was determined without reduction. The concentration of As(V) was calculated as a difference between As(total) and As(III).

Speciation modeling was performed with the program PHREEQC-2 (Parkhurst and Appelo 1999). Thermodynamic data for complexes and minerals of arsenic were compiled from the Minteq, Wateq and Llnl databases available with the PHREEQC-2. Data for Ca-bearing arsenic complexes and for Ca-arsenate minerals were taken from Bothe and Brown (1999) and data for Mg-bearing arsenic complexes from Whiting (1992).

Seven solid phase samples from upper ca. 5 cm were taken for stream sediment analyses by X-ray fluorescence (XRF) and five additional samples for sequential extraction. Samples for sequential extraction were taken at the borehole screen midpoint to enable a comparison between ground water concentration and solid phase concentration.

Modified sequential extraction similar to that performed by Bhattacharya et al. (2006) was performed with the following steps: (1) water-soluble fraction using de-ionized water (DIW), (2) exchangeable and carbonate fraction using 0.1 M sodium acetate $C_2H_3NaO_2$, (3) reducible fraction using 0.1 M hydroxylamine and HCl, (4) organic and sulfidic fraction using 8.8 M H_2O_2 and 1 M NH_4COOH, and (5) residual fraction using 7 M HNO_3.

Selected samples of the ore minerals and their weathering products were analyzed with a Cameca SX 100 electron microprobe, operated at 15 kV with a beam current of 20 nA. The counting times were 20 s for each element except As(30 s) and Pb(40 s). The following X-ray lines and standards were used: Si Kα-wollastonite, Al Kα-orthoclase, Pb Mα-PbS, Fe Kα, S Kα-$CuFeS_2$, Sb Lβ-Sb_2S_3, As Kβ-FeAsS, Mn Kα-Mn, Ca Kα-apatite.

Mike Zero software package (DHI 2004) was used for groundwater, surface water, and particle tracking modeling. Mike SHE was used for groundwater and particle tracking modeling, and Mike 11 for coupled surface water modeling. Data for the model were prepared, stored and further analyzed with Arc MAP-GIS software (ESRI 2004). The ground water heads and discharges from the mine tailings were measured and used for calibration and water balance calculations.

Results

Water chemistry

Field parameters and major ion chemistry

A summary of selected field parameters and ion concentrations are presented in Table 1. Values of pH in boreholes located in the mine tailing ponds (PK-7 and PK-8) are >6.6, suggesting significant neutralization by dissolution of carbonates. Values of Eh are in the range from +145 to +447 mV (lower values were measured under higher water table conditions). Concentrations of SO_4^{2-} in mine tailings are frequently high and reach 3,965 mg/L in borehole PK-8. In boreholes located in the mine tailings, most of iron concentration appears in the form of Fe(II) and the maximum concentration of total dissolved Fe reaches 143 mg/L in PK-7.

The boreholes located in the alluvium between the Blatina Creek and the mine tailing ponds have pH values also close to neutrality while Eh is slightly higher (up to +477 mV in PK-2) than in the mine tailings. The concentrations of the principal ions are much lower than SO_4^{2-} concentration and never exceed 300 mg/L. Concentrations of dissolved Fe are still relatively high, with a maximum of 23.5 mg/L in PK-2.

Values of pH in the Blatina Creek are always >7.5 (Table 1). The background value of SO_4^{2-} in sample SW-1 is 101.2 mg/L. However, in the zone affected by the mine drainage it may reach values greater than 100 mg/L (118.5 mg/L in sample SW-11), but it drops below 104.1 mg/L in sample SW-12 at the southern limit of the site. Concentrations of total Fe in the creek are almost always below 1 mg/L and background concentration at the non-contaminated site SW-1 is 0.77 mg/L.

Dissolved arsenic and antimony concentrations

Spatial distribution of the concentrations of dissolved arsenic at Pezinok is presented in Fig. 2 and the corresponding values are in Table 1. The vicinity of the mine tailing ponds is strongly contaminated.

The highest dissolved arsenic concentration was found in boreholes directly located in the mine tailing ponds (PK-7: up to 90,000 μg/L and PK-8: up to 28,700 μg/L). The maximum concentration of antimony found corresponded to borehole PK-8 (7,500 μg/L). No analytical speciation of antimony has been performed, but based on redox conditions, it is conjectured that antimony is present mostly as Sb(V).

Groundwater from the mine tailing ponds flows to the northern side of the tailing pond and into the drainage system at the southern part of the tailing pond. The analyses confirm a very high level of groundwater contamination with concentrations of As up to 27,380 μg/L, and Sb up to 7,750 μg/L at the discharge point GS-7. The highest concentration of arsenic in the alluvial aquifer out of the mine area was found on the right (west) side of the Blatina Creek alluvium, in borehole PK-2, where the arsenic and antimony concentrations reached 215 and 426 μg/L, respectively. On the other hand, concentrations of As and Sb in the PK-1 borehole, located further to the south, were close to the background concentrations.

The highest concentrations of As (104 μg/L) and of Sb (645 μg/L) in surface water were found in the mine water discharging from the Pyritova adit (MD-1). Analyses of water from Blatina Creek (Table 1; Fig. 2) sampled south of the tailing ponds demonstrate a strong attenuation of As and Sb contamination. Typical background concentrations of As and Sb in the surface water upstream from the site are 12 and 4 μg/L, respectively. In the area affected by the mine drainage, the As concentration ranges from 48 to 96 μg/L while the Sb concentration is from 25 to 67 μg/L (Table 1).

Based on the pe-pH diagrams and the results of As speciation on the amenable samples, dissolved arsenic is present exclusively as As(V). In Fig. 3a, the pe and pH values are based on the sampling in April 2004, when some water samples fell to the stability field of $H_2AsO_4^-$, but more samples were located in the stability field of $HAsO_4^{2-}$. Similar results are observed for data from November 2004 (Fig. 3b) at the end of the dry season.

Solid phase composition

Arsenopyrite in solid phase samples was identified by both optical microscopy and electron microprobe analysis. In the shallow oxidized zone of mine tailings (grayish to orange color of sediment) arsenopyrite grains were

Table 1 Field parameters and concentrations of dissolved species

Sampling points	*T* (°C)	EC (mS/m)	pH	Eh (mV)	Ca (mg/L)	Mg (mg/L)	Fe (mg/L)	Mn (mg/L)	HCO_3^- (mg/L)	SO_4^{2-} (mg/L)
MD-1	9.1	174.4	7.99	334	429.0	136.9	0.90	0.43	200.6	883.5
MD-2	9.3	82.1	7.48	471	98.7	74.5	3.78	1.57	169.1	216.0
MD-3	11.2	87.3	6.87	337	136.0	53.2	5.36	3.28	195.3	390.5
PK-1	13.4	74.8	6.95	423	99.7	37.2	20.3	0.493	196.7	209.4
PK-2	15.4	91.3	6.92	477	107.7	40.3	23.5	0.527	227.5	289.2
PK-3	11.1	59.1	6.87	407	68.5	24.4	9.27	0.687	150.7	169.5
PK-4	11.8	69	6.87	381	85.6	29.3	5.03	0.452	181.4	211.9
PK-5	16.6	67.8	7.14	447	83.5	28.7	2.78	0.277	267.5	155.1
PK-7	15.4	508	6.7	164	825.7	311.0	143.0	6.400	478.8	3,305
PK-8	14.9	563	4.03	145	960.7	820.0	60.0	1.920	197.0	3,965
Well	12.8	99.7	7.57	506	118.8	30.5	0.72	0.033	200.6	104.1
GS-2	13.9	212.0	8.07	368	804.9	150.3	7.74	2.790	292.5	1,125.8
GS-7	17.2	365.0	7.00	463	627.0	514.0	38.1	1.320	200.1	2,327
MW-5	9.5	178.5	7.15	217	233.6	91.6	5.48	1.500	316.0	774.4
MW-6	9.7	190.2	7.37	192	261.8	119.1	3.38	1.110	246.2	958.7
MW-10	13.1	86.5	7.56	472	109.7	44.6	0.87	1.290	129.1	354.7
SW-1	11.7	45.6	7.82	470	71.2	18.9	0.770	0.040	141.4	101.2
SW-8	11.6	39.9	7.77	254	50.3	16.5	0.477	0.074	86.2	100.4
SW-11	11.6	72.3	7.66	360	54.3	16.5	0.480	0.129	95.4	118.5
SW-12	11.1	41.4	7.86	334	51.3	15.8	0.500	0.094	95.4	104.1

Sampling points	Cl^- (mg/L)	NO_3^- (mg/L)	Al (μg/L)	As (μg/L)	Sb (μg/L)	Co (μg/L)	Cu (μg/L)	Ni (μg/L)	Zn (μg/L)
MD-1	21.2	11.3	90	104	645	49	<2	49	24
MD-2	6.0	9.3	40	29	150	8	<2	73	81
MD-3	6.2	1.5	30	33	46	37	<2	158	257
PK-1	13.4	7.2	1,220	16	15	4	<2	17	36
PK-2	7.6	0.9	4,990	215	426	4	<2	28	59
PK-3	6.0	2.3	1,320	79	22	<2	<2	16	83
PK-4	7.3	12.1	280	97	40	<2	<2	10	56
PK-5	33.3	7.5	360	16	18	<2	<2	5	11
PK-7	62.3	1.3	560	90,000	920	<2	<2	25	30
PK-8	131.8	1.4	120	28,700	7,500	<2	<2	52	30
Well	148.3	39.2	19	11	13	<2	<2	4	142
GS-2	7.1	8.3	40	2,830	750	<2	<2	12	86
GS-7	57.0	2.1	60	27,380	7,750	<2	<2	47	53
MW-5	15.8	11.5	<30	2,200	286	<2	<2	9	26
MW-6	30.2	10.8	60	900	900	<2	<2	28	23
MW-10	6.9	4.7	<30	42	139	<2	<2	18	19
SW-1	11.2	14.5	80	12	4	<2	<2	11	18
SW-8	11.6	10.3	80	96	38	<2	3	13	20
SW-11	11.8	11.9	80	48	39	<2	<2	15	22
SW-12	12.0	9.5	80	93	45	<2	3	13	19

corroded, with reaction rims found on the surface (Fig. 4a). These rims have a high Fe content, reaching up to 36.35 wt% (minimum 31.71 wt%, average 34 wt%). Content of As in reaction rims was up to 19.06 wt% (minimum 14.22 wt%, average 17.1 wt%). There is also a relatively high Sb content in the weathering rims (6.04 wt% in average; maximum 9.46 wt%), exceeding the Sb content in primary arsenopyrite (max. 0.05 wt%). This indicates that the antimony source is not arsenopyrite and is presumably coming from minerals like stibnite and berthierite. A

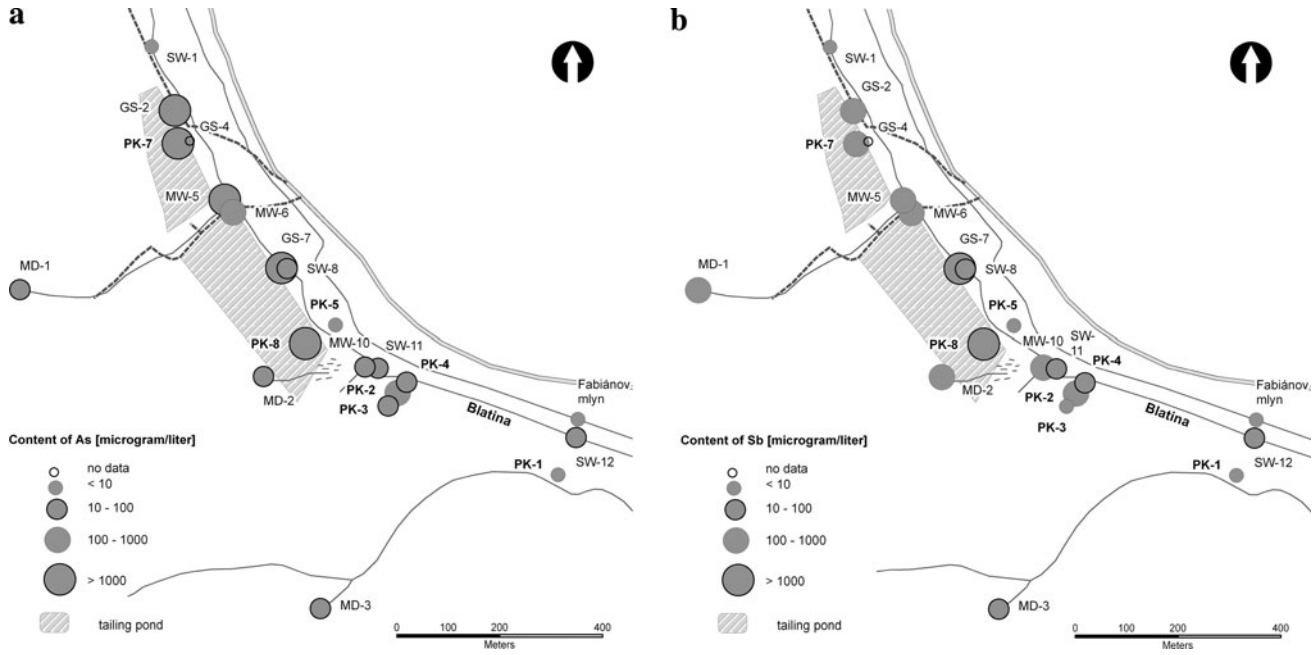

Fig. 2 Map of concentrations of dissolved arsenic (**a**), map of concentrations of dissolved antimony (**b**)

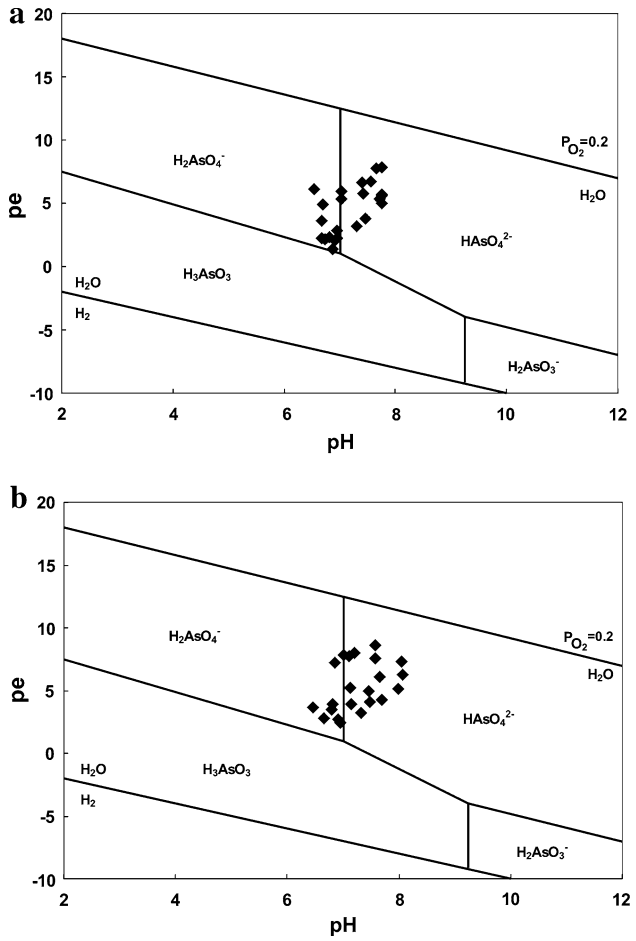

Fig. 3 pe-pH diagrams for dissolved arsenic: **a** April 2004, **b** November 2004

remarkable feature of the reaction rims is a significant negative correlation ($R = -0.84$) between As and Sb (Fig. 5).<Dummy RefID="Fig5

The most abundant ore mineral of the tailings is pyrite, where the enrichment of the weathering rims is also evident. The As content in the surface weathering rims of pyrite ranges from 0 to 5.33 wt% while in the case of Sb it can be up to 7.5 wt%.

In the deeper, unoxidized zone (gray color of sediment), the arsenopyrite and pyrite grains appear fresh, with idiomorfic and hypidiomorfic crystals.

Stibnite was found only in the deeper sediments. This mineral has dissolved quickly in shallow sediments, probably as a consequence of its low stability compared to arsenopyrite and pyrite. It is assumed that this mineral was a principal source of Sb in reaction rims on arsenopyrite.

Berthierite seems to be more recalcitrant than stibnite, but its presence is relatively rare. There are also reaction rims on berthierite grains (Fig. 4b), with Fe contents of about 28.76 wt% and Sb about 20.73 wt%. Its As content is about 6.84 wt%.

Degree of alteration for various sulfidic minerals in the mine tailings was assessed using a standard optical microscope. The degree of alteration in mine tailings decreases in the order stibnite > arsenopyrite > pyrite.

The results of the sequential mineral extraction are shown in Table 2. Sample PK-1 represents a site with a minimum contamination located downstream from tailing ponds (close to Fabianov mlyn; Fig. 1). There, the total As content in the solid phase is 168 mg/kg and most of it is in

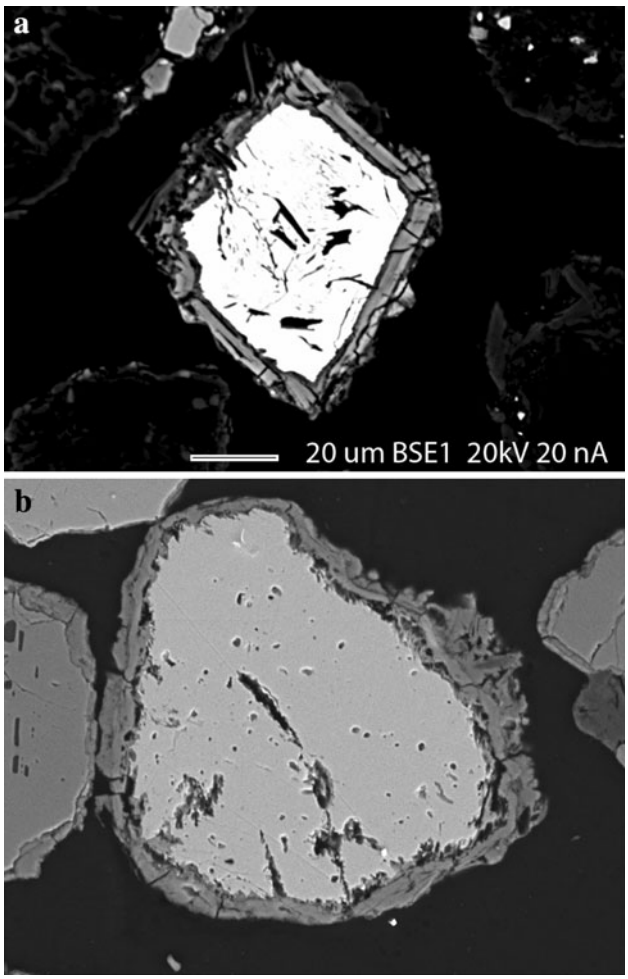

Fig. 4 Electron microprobe images in BES mode: Weathering rims on arsenopyrite (**a**), and bethierite (**b**) grains

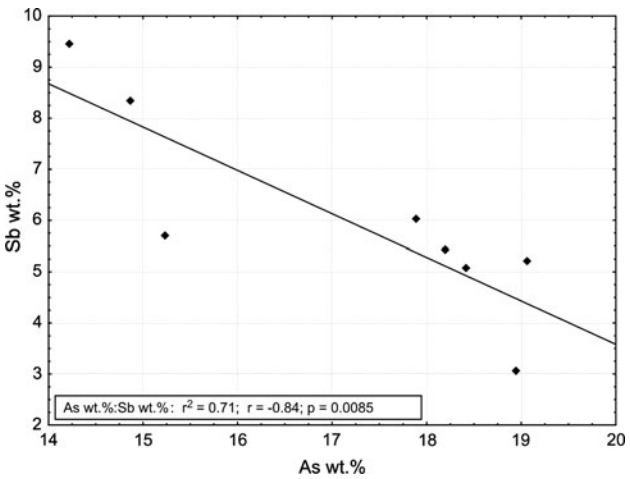

Fig. 5 Graph of As versus Sb content in reaction rims, R is Pearson's correlation coefficient, R^2 is coefficient of determination

the residual fraction (159 mg/kg). A non-negligible content of 7.2 mg/kg is in the reducible fraction, which potentially represents the As adsorbed onto the surface of ferric oxide and hydroxides. Sample PK-4 is located closer to tailing ponds than PK-1 (right bank of the Blatina Creek; Fig. 1). The total content of As is 113 mg/kg, which is lower than in the PK-1 sample. However, the As content associated with the reducible fraction is higher, reaching 14.5 mg/kg. Samples PK-6 and PK-8 are both from the shallow oxidized zone of boreholes located directly in the southern tailing pond (Fig. 1). The total content of As is higher (6,262 and 10,850 mg/kg, respectively) and the maximum contents of As are in the residual fraction (i.e. bound to oxy-hydroxides), the oxidizable fraction (i.e. bound to sulfides and organic matter), and the reducible fraction (i.e. bound to silicates). The As content in the reducible fraction of sample PK-8 is 5,700 mg/kg. This suggests a significant weathering of arsenopyrite present in the sediments. However, in sample PK-6, the As reducible fraction is significantly smaller (908 mg/kg). In both samples, there is a large pool of oxidizable and residual As, suggesting potential for on-going, long-term oxidation of arsenopyrite. Finally, sample PK-7 was taken from a shallow zone of the northern tailing pond (Fig. 1). Total As content, 4,851 mg/kg, is lower than in the samples from the southern tailing pond. Arsenic is almost equally distributed among reducible (1,364 mg/kg), oxidizable (1,645 mg/kg), and residual (1,586 mg/kg) fractions. The Sb content of Sb (Table 2) follows the same pattern as As content (e.g., maximum values in residual, oxidizable, and reducible fractions), but values are generally lower. The highest total contents of Sb are in samples PK-6, PK-7, and PK-8 from mine tailings with respective values of 5,523, 4,023, and 8,710 mg/kg. Samples PK-1 and PK-4 taken out of mine tailings have much lower Sb contents, but respective values of in reducible (i.e. oxy-hydroxides) fraction 4.0 and 0.7 mg/kg are not negligible.

The content of total As and Sb in stream sediments of the Blatina Creek are presented in Fig. 6. Sample S-1 with As content of 78 mg/kg and Sb content of 45 mg/kg represents background conditions upstream from the tailings. Sample S-2 is still unaffected by AMD (As = 95 mg/kg; Sb = 24 mg/kg) although its impact becomes evident in Sample S-3 (As = 484 mg/kg; Sb = 100 mg/kg) close to the southern tailings pond. Samples S-4 S-5 have the highest As and Sb contents (1,213/201 and 1,017/359 mg/kg, respectively) and they are strongly affected by contaminant input from ground water discharge at sites GS-7 and MW-10 (Fig. 1). Samples S-6 and S-7 have declining contents (As = 642; Sb = 173 mg/kg in sample S-7 at the southern edge of the site). Maximum As and Sb contents in samples S-4 and S-5 also correspond to increased contents of Fe and Mn in the solid phase. This suggests adsorption on Fe- and Mn-oxyhydroxides precipitated in the creek, which has been confirmed by mineralogical analyses (Trtikova 1999; Trtikova et al. 1997; Majzlan et al. 2007).

Table 2 Results of sequential extraction

Borehole	PK-1		PK-4		PK-6		PK-7		PK-8	
Depth (cm)	500–540		520–260		1,300–1,333		780–800		780–800	
Sample	(mg/kg)	%	(mg/kg)	%	(mg/kg)	%	(mg/kg)	%	(mg/kg)	%
As 1	0.7	0.4	1.7	1.5	38.2	0.6	26.9	0.6	90.9	0.8
As 2	<0.1	0	<0.1	0	146	2.3	229	4.7	233	2.1
As 3	7.2	4.3	14.5	12.8	908	14.5	1.364	28.1	5.700	52.7
As 4	0.6	0.4	1.7	1.5	2.095	33.5	1.645	33.9	1.535	14.1
As 5	159	94.9	95.1	84.2	3.075	49.1	1.586	32.7	3.291	30.3
As total	168	100	113	100	6.262	100	4.851	100	10.850	100
Sb 1	1.2	0.4	2.3	8.3	424	7.7	242	6.0	353	4.1
Sb 2	<0.1	0	<0.1	0	<0.1	0	<0.1	0	<0.1	0
Sb 3	4.0	1.2	0.7	2.5	784	14.2	323	8.0	612	7.0
Sb 4	0.6	0.2	0.3	1.1	77	1.4	27.9	0.7	50.7	0.6
Sb 5	321	98.2	24.5	88.1	4.238	76.7	3.430	85.3	7.694	88.3
Sb Total	327	100	27.8	100	5.523	100	4.023	100	8.710	100

1 water-soluble fraction, *2* exchangeable and carbonate fraction, *3* reducible fraction, *4* organic and sulfidic fraction, *5* residual fraction, *T* total content

Speciation calculations

Speciation modeling has been performed using PHREEQC-2 (Parkhurst and Appelo 1999). Saturation indices for several minerals including calcite, rhodochrosite, gypsum, amorphous $Al(OH)_3$, and $Fe(OH)_3$, goethite, siderite, and scorodite were obtained from PHREEQC-2 calculations (Table 3).

Amorphous $Fe(OH)_3$ has positive saturation index values for most of the studied waters. In all cases the SI for goethite was positive. The formation of goethite by transformation and maturation of metastable phases like ferrihydrite is common at the Pezinok site according to the findings related to the mineralogical characterization of ochre phases (Trtikova 1999). It is assumed that in surface streams the metastable phases are more common (Majzlan et al. 2007). On the other hand, goethite was identified in some samples obtained from boreholes PK-7 and PK-8, which are located directly in the tailings pond. All the water samples were undersaturated with respect to scorodite. It appears that the saturation is not reached because Fe(III) concentrations are relatively low due to high pH conditions.

Because of the supersaturation of water with respect to amorphous $Fe(OH)_3$ and goethite, we conjecture that adsorption onto these phases may constrain the dissolved arsenic and antimony concentrations. The concentration of dissolved manganese may be controlled by the precipitation of rhodochrosite (Sracek et al. 2004) because positive values of SI were found only for water samples from the PK-7 borehole. Based on mineralogical analyses and speciation calculation results, the presence of any particular secondary arsenic and antimony minerals is not probable.

High concentrations of sulfate and bicarbonate were found in ground water from boreholes PK-7 and PK-8 where SI are in equilibrium or close to equilibrium with calcite and gypsum. The saturation with respect to gypsum is consistent with high observed concentration of dissolved sulfate (Table 1). According to the results of mineralogical analyses, the precipitation of gypsum is evident in the surrounding of the mine tailing ponds, and not only in water from boreholes located directly in the mine tailing ponds.

Ground water in the alluvium of the Blatina Creek is supersaturated with respect to siderite, except for borehole PK-5, which is located at the left side of the creek.

Saturation indices for Ca-arsenates were calculated only for water samples from the mine tailings with very high dissolved As(V) concentrations. All SI values were negative, indicating undersaturation with respect to these mineral phases.

Groundwater flow

The purpose of the flow modeling was to determine arsenic transport out of mine tailings and the contribution of arsenic-rich ground water to the discharge in the Blatina Creek. The first step in the flow model preparation was the creation of a conceptual model of the area. From the modeling point of view, we assume that the aquifer is composed of alluvial sediments of Blatina Creek. The

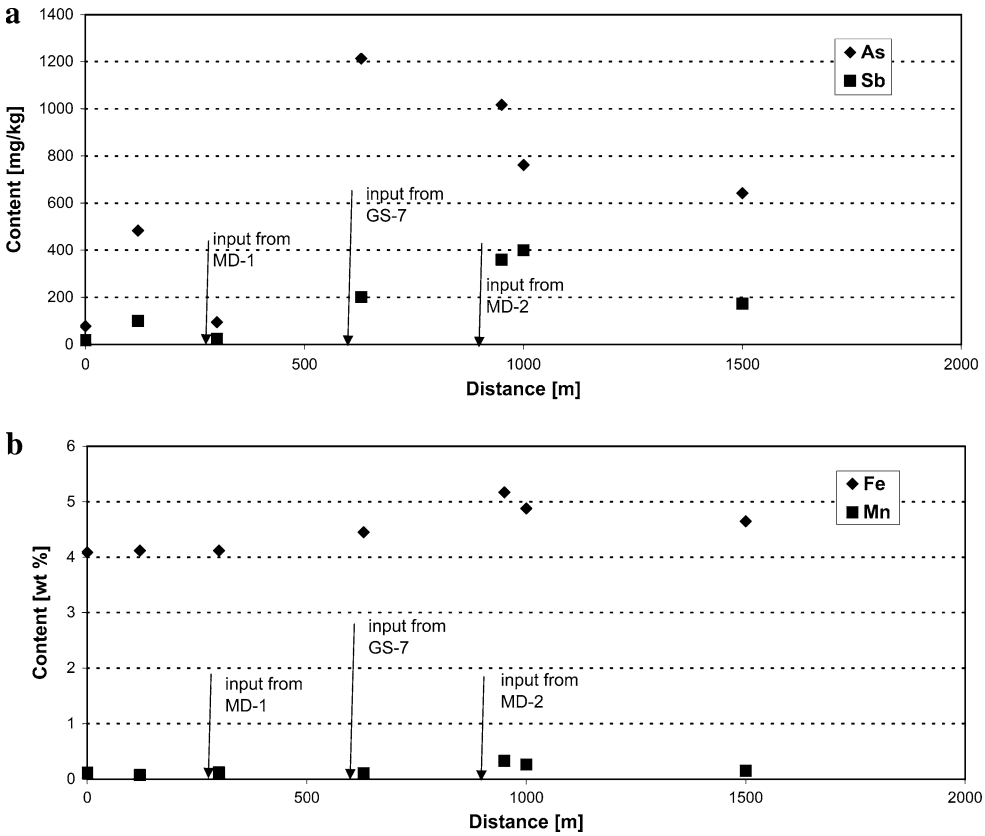

Fig. 6 Total contents at surface of stream sediments of the Blatina Creek: **a** As and Sb, **b** Fe and Mn, location of input from mine adits tributaries is indicated by *vertical arrows*

aquifer is confined, with an average thickness of 4 m. The average hydraulic conductivity is 5×10^{-4} m/s based on granulometric curves and pumping tests (Chovan et al. 2006). The boundary conditions were set to constant head at the boundaries of the modelling domain where the creek is entering and leaving the study site and constant flow elsewhere. The upper boundary condition on the Blatina Creek is constant flow and lower boundary condition is a constant head whose value was established according to measurements done in the field.

The system was modeled under steady state flow regime and water level measurements from observation wells and water flow from the Blatina Creek were used as calibration targets. The principal uncertainty in the data was in the assumed hydraulic conductivity, the height of the bottom of the aquifer, and the leakage coefficient associated to the riverbed sediments. Best guesses of these values were initially given to the model and further refined during the calibration stage. The calibration target was set to around 15 cm of maximum error in hydraulic heads (Chovan et al. 2006).

According to the results of the model, ground water flows from the neighboring uphill through from the mine tailings pond, mostly in its southern tip, then after reaching alluvial sediments changes its direction from southeast towards the south. Then, ground water flows nearly parallel to the Blatina Creek and after approximately 150 m recharges the creek (Fig. 7). The particle tracking simulation based on advective transport also confirmed the results: particles initially located at the eastern boundary of mine tailings are transported in the alluvial aquifer in the direction parallel to the Blatina Creek and enter the creek southeast of mine tailings.

Averaged inflow of ground water, which passed through mine tailing ponds, into the Blatina Creek at the seepage face south of the mine tailings is 2.0×10^{-3} m^3/s at high flow period (early Spring) and 2.5×10^{-4} m^3/s at low flow period (late Summer). This is much less than the minimum surface water discharge in the Blatina Creek, which is about 0.1 m^3/s. The mass flux of arsenic into the Blatina Creek is for the minimum discharge in the creek and during dry periods arsenic concentration of 93 μg/L (based on data from November 2004, Table 1) are equivalent to 9.3 mg/s. On the other hand, mass flux of arsenic entering the creek by ground water discharge is about 54 μg/s during low flow periods with arsenic concentrations of about 215 μg/L found in the alluvial aquifer. Thus, the ground water sources of arsenic input comprises a very small fraction (about 0.6%) of total arsenic mass flux in the Blatina Creek and surface water sources of arsenic input from mine adits are much more important. Similar calculations for antimony gives mass flux in the Blatina Creek at approximately 4.5 mg/s and a mass flux for ground water

Table 3 Values of saturation indices for selected minerals

Sample	Date	Calcite	Rhodochrosite	Gypsum	Amorphous $Al(OH)_3$	Amorphous $Fe(OH)_3$	Goethite	Siderite	Scorodite
MD-1	April 04	0.43	−0.06	−0.56	−0.79	3.06	8.36	−2.11	−5.63
	Nov. 04	0.57	0.21	−0.81	−1.98	3.77	9.08	−1.36	−4.95
MD-2	April 04	−0.53	0.09	−1.28	−1.42	3.21	8.49	0.17	−5.23
	Nov. 04	−0.34	0.33	−1.32	1.46	3.63	8.93	0.55	−4.67
MD-3	April 04	−0.88	0.07	−1.01	−0.46	2.32	7.64	−0.02	−4.53
PK-1	April 04	−0.56	0.09	−1.20	0.67	−0.08	5.23	−0.21	−7.65
	Nov. 04	−0.67	−0.46	−1.26	1.06	4.57	9.95	−0.33	−3.25
PK-2	April 04	−0.66	−0.67	−1.21	0.70	0.04	5.38	0.18	−6.71
	Nov. 04	−0.92	−0.36	−1.54	0.38	1.48	6.90	1.04	−5.06
PK-3	April 04	−1.04	−0.60	−1.51	1.09	−0.29	5.08	0.43	−6.97
	Nov. 04	−0.96	−0.70	−1.43	0.26	1.85	7.23	0.22	−4.76
PK-4	April 04	−0.93	−0.69	−1.28	0.37	−0.31	5.06	0.00	−7.07
	Nov. 04	−0.77	−0.36	−1.29	0.43	1.25	6.65	0.21	−5.24
PK-5	April 04	−0.30	−0.46	−1.58	0.08	2.55	8.13	−0.79	−5.35
	Nov. 04	−0.31	−0.30	−1.60	0.31	2.44	7.84	0.42	−5.57
PK-7	April 04	0.06	0.57	0.00	0.24	0.70	6.19	1.42	−3.07
	Nov. 04	−0.02	0.32	0.18	−0.58	1.15	6.58	1.23	−2.58
PK-8	April 04	−0.38	−0.34	0.09	−0.19	1.05	6.56	0.88	−3.15
	Nov. 04	−0.10	−0.33	0.29	−1.19	1.53	6.95	0.91	−2.94
Well	April 04	0.18	−1.22	−1.46	−1.13	1.65	7.02	−4.20	−7.17
	Nov. 04	−0.28	−1.56	−1.91	−1.21	1.55	6.98	−6.37	−7.49
GS-2	April 04	0.04	0.05	−0.17	−0.99	0.77	6.10	−0.06	−4.45
	Nov. 04	0.99	−0.57	−0.49	−1.65	2.02	7.50	−4.24	−6.66
GS-4	April 04	−0.50	−1.74	−1.58	−1.63	2.01	7.33	−5.45	−6.71
GS-7	April 04	−0.14	−0.38	0.01	−1.35	1.72	7.33	0.73	−2.96
	Nov. 04	−0.37	−1.25	−0.12	−1.21	3.29	8.73	−3.06	−3.42
MW-6	April 04	0.11	−0.08	−0.46	−0.53	2.05	7.34	0.28	−4.48
	Nov. 04	0.08	0.28	−0.59	−0.71	2.30	7.59	0.48	−4.30
MW-10	Nov.04	−0.43	0.14	−1.00	−1.32	3.40	8.80	−3.18	−4.18
SW-1	April 04	−0.65	−1.39	−2.02	−0.97	3.15	8.50	−4.70	−5.52
	Nov. 04	−0.16	−0.91	−1.62	−1.65	3.50	8.90	−3.30	−5.26
SW-11	April 04	−0.56	−0.91	−1.69	−0.95	3.12	8.40	−2.12	−5.53
	Nov. 04	0.06	0.05	−1.28	−0.41	3.65	9.04	−1.79	−4.35

discharge at approximately 106 μg/s, comprising 2.3% of total antimony flux in the creek. Furthermore, the presented calculation results are for conservative transport and processes associated to the hyporheic zone. Adsorption on and co-precipitation with Fe(III)-oxyhydroxides may further reduce the dissolved As and Sb concentrations discharged by ground water (Ford 2005; Gandy et al. 2007; Hiller et al. 2009), decreasing the As and Sb loading into the surface water. However, arsenic and antimony may be re-mobilized in a creek when redox conditions change (Casiot et al. 2005). For example, photoreduction of Fe-oxyhydroxides during day light may increase concentrations of dissolved Fe and release adsorbed As and Sb (Gammons et al. 2008; Egal et al. 2010).

Discussion

In the Western Carphatians, the ground water background level concentrations of arsenic have been reported in the range from 0.5 to 116 μg/L in granitic rocks, from 0.5 to 94 μg/L in schists, from 8.5 to 887 μg/L in granitic rocks containing ore mineralization, and from 0.5 to 820 μg/L for schists containing ore mineralization (Rapant et al. 1996). Thus, the highest concentration of arsenic found at the Pezinok site is far beyond the reference range.

In mining wastes, a typical sequence of neutralization reactions involving the consumption of different minerals has been described (Jurjovec et al. 2002; Blowes et al. 2003). Fast-dissolving neutralization carbonate minerals,

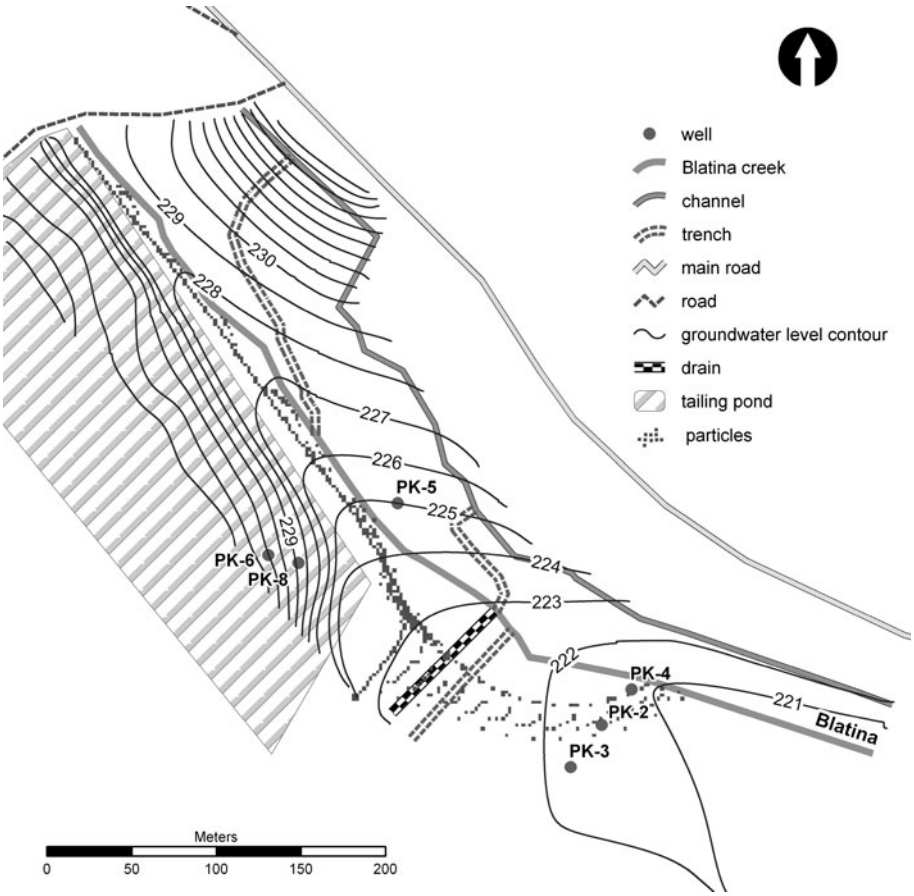

Fig. 7 Modeled flow pattern and particle tracking between mine tailing ponds and the Blatina Creek

like calcite, dissolve first and their dissolution keeps pH above 6.0. Once it has been depleted, the dissolution of siderite begins and keeps pH around 5.0. When siderite is gone, aluminum hydroxide and ferric hydroxide dissolve and their dissolution keep pH around 4.0 and 3.0, respectively. The processes listed above are relatively fast and are often approximated as equilibrium reactions. Significant dissolution of silicates, like chlorite and muscovite, starts only after the dissolution of hydroxides and pH is already low at this stage (sometimes around 2.0) because this process is kinetically constrained (Blowes et al. 2003).

In mine tailings ponds at the Pezinok site, pH values are above 6.0 due to high carbonate content in the gangue rocks and neutralization by the dissolution of carbonates is an on-going process. Initially, arsenopyrite is oxidized by oxygen in the unsaturated zone (Walker et al. 2006):

$$\mathrm{FeAsS} + 2.75\mathrm{O_2} + 1.5\mathrm{H_2O} = \mathrm{Fe^{2+}} + \mathrm{H_3AsO_3} + \mathrm{SO_4^{2-}} \quad (1)$$

Oxidation of arsenopyrite by Fe(III), which is important in low pH water (Yunmei et al. 2004), is not significant at Pezinok because Fe(III) concentrations have to be low due to high pH values. The reaction above does not directly generate acidity, but acidity is produced by the formation of ferric hydroxide, which precipitates on the surface of arsenopyrite grains,

$$\mathrm{Fe^{2+}} + 0.25\mathrm{O_2} + 2.5\mathrm{H_2O} = \mathrm{Fe(OH)_3} + 2\mathrm{H^+} \quad (2)$$

Acidity produced in this reaction is neutralized by dissolution of carbonates like calcite and, simultaneously, gypsum precipitates,

$$\mathrm{CaCO_3} + 2\mathrm{H^+} + \mathrm{SO_4^{2-}} = \mathrm{CaSO_4 \cdot 2H_2O} + \mathrm{H_2CO_3} \quad (3)$$

This means that a significant part of iron and sulfate, produced by the oxidation of arsenopyrite and other sulfides such as pyrite, remains in the mine tailings. Formation of rims composed of Fe(III) oxide and hydroxides probably limits the access of oxygen to the surface of unoxidized arsenopyrite and, thus, decreases arsenopyrite oxidation rate. Precipitation of the rims has been proven by mineralogical analyses (Fig. 4a, b). Simultaneously, in the presence of oxygen, As(III) is oxidized to As(V),

$$\mathrm{H_3AsO_3} + 0.5\mathrm{O_2} = \mathrm{HAsO_4^{2-}} + 2\mathrm{H^+} \quad (4)$$

This reaction also produces acidity, which is consumed by carbonate dissolution. As(V) present as $\mathrm{HAsO_4^{2-}}$ at

Table 4 As/Sb ratios and K_d values

Site	$(As/Sb)_{water}$	$(As/Sb)_{solid}$	K_d (L/kg)
PK-1	1.33	1.50	n.a.
PK-4	1.80	5.26	n.a.
PK-7*	117.8	2.86	n.a.
PK-8*	20.23	6.24	n.a.
As	n.a.	n.a.	61.2
Sb	n.a.	n.a.	254.7

n.a. not applicable

* Samples with dissolved As concentration >10 mg/l

pH > 7.0 is then adsorbed onto ferric hydroxides rims. Adsorption capacity for As(V) decreases with pH due to an increasingly negative surface charge of Fe(III)-oxyhydroxides, but it is still significant at a pH range 6.6–7.6 observed at certain sampling points at the Pezinok site (Stollenwerk 2003).

Data on the oxidation kinetics of stibnite are not available, however, at the Pezinok site it seems to be faster compared to arsenopyrite oxidation kinetics for two reasons: (1) in the shallow zone of mine tailings almost all stibnite has been dissolved, but arsenopyrite is still present, and (2) there is a zonality of Sb content in Fe(III) oxyhydroxide rims with maximum Sb contents close to primary sulfide grains, i.e. in rims formed in the early stage of mine tailings oxidation (Chovan et al. 2006).

Adsorption of As(V) may also be limited by the competition with Sb(V) for adsorption sites. As for other oxyanion forming elements, adsorption of antimony species decreases with increasing pH, (Krupka and Serne 2002). An evidence for the competition with Sb(V) for adsorption sites is supported by negative correlation between As and Sb contained in reaction rims on the weathering surface of arsenopyrite grains (Fig. 5). However, when concentrations of As(V) and Sb(V) in water are comparable, adsorption affinity of As(V) for Fe(III) oxide and hydroxides is generally higher (Ashley et al. 2003). Also, amorphous Fe(III) and Mn(IV) oxide and hydroxides may oxidize Sb(III) to Sb(V) and increase adsorption affinity for antimony. The As/Sb ratios and calculated K_d values are shown in Table 4. The As/Sb ratios for both water and solids based on the data from sequential extraction (first 3 steps, i.e. relatively easily available fractions) and sampling of ground water from wells are always higher than 1.0, however, in samples from mine tailings with extremely high dissolved As concentrations (PK-7, PK-8) the ratio in solid phase is at least one order of magnitude lower than in water [for example, in sample PK-7 $(As/Sb)_w$ is 117.8 and $(As/Sb)_s$ is only 2.86]. This is also reflected by lower values of the linear adsorption isotherm K_d for arsenic than for antimony (61.1 and 254.7 L/kg, respectively). This is different from reported results (for example, Casiot et al. 2007), however, the discrepancy may have been caused by limited number of samples, heterogeneous initial distribution of arsenopyrite and stibnite or, most probably, by the non-linear behavior of the adsorption phenomena (Freundlich or Langmuir type isotherms) at this high water concentrations. However, this cannot be verified due to the lack of data in the intermediate concentration range.

Adsorption seems to be the principal arsenic and antimony attenuation process, but biological processes such as incorporation of arsenic into plants may also play a role. Saturation indices for all Ca-arsenates were negative. At the Pezinok site most dissolved As is present as As(V). This is different from what was obtained in controlled laboratory experiments on the reaction of As-sulfides by oxygen (for example, Lengke and Tempel 2003; Walker et al. 2006), where about 60% of As was present as As(III). This may probably be explained by a longer time available for As(III) oxidation in the field compared to laboratory column experiments (Table 1).

Conclusions

The Pezinok site is contaminated by arsenic. Investigation of this site based on sampling of pore water in mine tailings, ground water in surrounding aquifer and surface water, mineralogical analyses, and flow and geochemical modeling revealed the extent of contamination and identified natural attenuation processes. The highest dissolved arsenic concentrations (up to 90,000 μg/L) were found in mine tailings with arsenic occurring predominately as As(V). Concentrations of dissolved antimony in mine tailings were up to 7,500 μg/L.

The primary arsenic source is the weathering of arsenopyrite. Pore water in the mine tailings is well-buffered by dissolution of carbonates (pH values are between 6.6 and 7.0) and arsenopyrite grains are surrounded by reaction rims composed of ferric iron minerals. There is a high content of As (average value 17.1 wt%) and Sb (average value 6.04 wt%) incorporated into the reaction rims. A significant negative correlation between As and Sb contents suggests that competition for adsorption sites with Sb(V), produced by the oxidation of stibnite, limits the adsorption of As(V). Based on the sequential extraction results, most of the solid phase arsenic is in reducible fraction (e.g. adsorbed on ferric oxide and hydroxides), sulfidic fraction and in residual fraction. The distribution of antimony revealed by sequential extraction is similar, but total contents are lower. The rate of arsenopyrite oxidation is probably limited by the formation of ferric mineral rims

on its surface, which prevents penetration of oxygen to the un-oxidized arsenopyrite.

Water in mine tailings is at equilibrium with gypsum and calcite, but not at equilibrium with any arsenic mineral. Gypsum incorporates calcium produced by the dissolution of carbonates. Concentrations of dissolved arsenic in surrounding aquifer are much lower, with respective arsenic and antimony concentrations up to 215 and 426 μg/L. Arsenic and antimony are transported from mine tailings by ground water flow towards the Blatina Creek, however their total ground water loadings are relatively low (about 0.6% for As and about 2.3% for Sb) compared to surface water contaminant sources. In the Blatina Creek, arsenic and antimony are attenuated by dilution and adsorption on ferric iron minerals in stream sediments with resulting respective dissolved concentrations 93 and 45 μg/L at southern limit of the site.

Acknowledgments The research was based on the results of the Slovak Research and Development Agency under the contract No. APVV-0268-06 "Contamination generated by Sb mining in Slovakia: Evaluation and strategies for remediation". We thank an anonymous reviewer whose comments helped to improve the manuscript. We also thank Angus Calderhead for language editing.

References

Ahmed KM, Bhattacharya P, Hasan MA, Akhter SH, Alam SMM, Bhuyian MA, Imam MB, Khan AA, Sracek O (2004) Arsenic enrichment in groundwater of the alluvial aquifers in Bangladesh: an overview. Appl Geochem 19:181–200

Armienta MA, Segovia N (2008) Arsenic and fluoride in the groundwater of Mexico. Environ Geochem Health 30(4): 345–353

Armienta MA, Villasenor G, Rodrigues R, Ongley LK, Mango H (1993) The role of arsenic-bearing rocks in groundwater pollution at Zimapan Valley, Mexico. Environ Geol 40:571–581

Ashley PM, Craw D, Graham BP, Chapell DA (2003) Environmental mobility of antimony around mesothermal stibnite deposits, New South Wales, Australia and southern New Zealand. J Geochem Explor 77:1–14

Bhattacharya P, Claesson M, Bundschuh J, Sracek O, Fagerberg J, Jacks G, Martin RA, del Storniolo A, Thir JM (2006) Distribution and mobility of arsenic in the Río Dulce alluvial aquifers in Santiago del Estero Province, Argentina. Sci Tot Environ 358:97–120

Blowes DW, Ptacek CJ, Jambor JL, Weisener CG (2003) The geochemistry of acid mine drainage. In: Lollar BS (ed) Environmental geochemistry, vol 9, treatise on geochemistry. Elsevier, Amsterdam, pp 149–204

Bothe JV, Brown PW (1999) The stabilities of calcium arsenates at 23 ± 1°C. J Hazard Mater 69:197–207

Cambel B (1959) Hydrothermal deposits in the Malé Karpaty Mts., mineralogy and geochemistry of their ores (in Slovak). Acta Geol Geogr Univ Comen Geol 3:1–348

Casiot C, Lebrun S, Morin G, Bruneel O, Personné JC, Elbaz-Poulichet F (2005) Sorption and redox processes controlling arsenic fate and transport in a stream impacted by acid mine drainage. Sci Tot Environ 347:122–130

Casiot C, Ujevic M, Munoz M, Seidel JL, Elbaz-Poulichet F (2007) Antimony and arsenic in a creek draining an antimony mine abandoned 85 years ago (Upper Orb basin, France). Appl Geochem 22:788–798

Chovan M, Rojkovič I, Andráš P, Hanas P (1992) Ore mineralization of the Malé Karpaty Mts. Geol Carpath 43:275–286

Chovan M, Háber M, Jelen S, Rojkovic I et al (1994) Ore textures in the Western Carpathians. Slovak Academic Press, Bratislava

Chovan M, Andráš P, Čerňanský S, DlapaP, Fľaková R, Hudáček M, Krčmář D, Kušnierová M, Lalinská B, Lux A, Majzlan J, Milovská S, Moravanský D, Ševc J, Šimoničová A, Šlesárová A, Šottník P, Uhlík P, Urík M, Ženišová Z (2006) Stanovenie rizika kontaminácie okolia Sb, Au, S ložiska Pezinok a návrh na remediáciu: toxicita As a Sb, acidifikácia. (In Slovak: Determination of the contamination risk by Sb, As, S around the Pezinok ore deposit and remediation proposal: toxicity of As and Sb, acidification), final report of the project of MŠ SR, no. AV/901/2002 (VTP25). Manuscript, Faculty of Science, Comenius University, Bratislava, p 225

DHI (2004) Mike SHE. An integrated hydrological modelling system, users guide. Danish Hydrological Institute, p 377

Donahue R, Hendry MJ (2003) Geochemistry of arsenic in uranium mine mill tailings, Saskatchewan, Canada. Appl Geochem 18:1733–1755

Egal M, Casiot C, Morin G, Elbaz-Poulichet F, Cordier MA, Bruneel O (2010) An updated insight into the natural attenuation of As concentrations in Regious Creek (southern France). Appl Geochem 25:1949–1957

ESRI (2004) What is Arc GIS, GIS by ESRI, p 76

Filella M, Belzile N, Chen Y-W (2002) Antimony in the environment: a review focused on natural waters, I. Occurrence. Earth Sci Rev 57:125–176

Flakova R, Zenisova Z, Drozdova Z, Milovská S (2005) Distribution of arsenic in surface and groundwater in Kolarsky vrch mining area (Male Karpaty Mts.) (in Slovak). Podzemna voda 11:90–103

Ford R (2005) The impact of ground-water/surface-water interactions on contaminant transport with application to an arsenic contaminated site. EPA/600/S-05/002. http://www.epa.gov/nrmrl/pubs/600s05002/epa_600_s05_002.pdf. Accessed 22 Dec 2010

Gammons CH, Nimick DA, Parker SR, Snyder DM, McCleskey RB, Amils R, Poulson SR (2008) Photoreduction fuels biogeochemical cycling of iron in Spain's acid rivers. Chem Geol 252:202–213

Gandy CJ, Smith JWN, Jarvis AP (2007) Attenuation of mining-derived pollutants in the Hyporheic zone: a review. Sci Tot Environ 373:435–446

Giere R, Sidenko NV, Lazareva EV (2003) The role of secondary minerals in controlling the migration of arsenic and metals from high-sulphide wastes (Berikul gold mine, Siberia). Appl Geochem 18:1347–1359

Hiller E, Jurkovic L, Kordik J, Slaninka I, Jankular M, Majzlan J, Göttlicherd J, Steiningerd R (2009) Arsenic mobility from anthropogenic impoundment sediments—consequences of contamination to biota, water and sediments, Posa, Eastern Slovakia. Appl Geochem 24:2175–2185

Juillot F, Ildefonse Ph, Morin G, Calas G, de Kersabiec AM, Benedetti M (1999) Remobilization of arsenic from buried wastes at an industrial site: mineralogical and geochemical control. Appl Geochem 14:1031–1048

Jurjovec J, Ptacek CJ, Blowes DW (2002) Acid neutralization mechanisms and metal release in mine tailings: a laboratory column experiment. Geochim Cosmochim Acta 66:1511–1523

Kopřiva A, Zeman J, Sracek O (2005) High arsenic concentrations in mining waters at Kaňk, Czech Republic. In: Bundschuh J, Bhattacharya P, Chandrasekharam (eds) Natural arsenic in

groundwater: occurrence, remediation and management. A.A. Balkema Publishers, Amsterdam, pp 49–56

Krupka KM, Serne RJ (2002) Geochemical factors affecting the behavior of antimony, cobalt, europium, technetium, and uranium in vadose sediments. Report PNNL-14126. Pacific Northwest National Laboratory

Langmuir D, Mahoney J, MacDonald A, Rowson J (1999) Predicting arsenic concentrations in the porewaters of buried uranium mill tailings. Geochim Cosmochim Acta 63:3379–3394

Langmuir D, Mahoney J, Rowson J (2006) Solubility products of amorphous ferric arsenate and crystalline scorodite ($FeAsO_4{\cdot}2H_2O$) and their application to arsenic behavior in buried mine tailings. Geochim Cosmochim Acta 70:2942–2956

Lengke MF, Tempel RN (2003) Natural realgar and amorphous AsS oxidation kinetics. Geochim Cosmochim Acta 67:3281–3291

Majzlan J, Lalinská B, Chovan M, Jurkovic L, Milovska S, Göttlicher J (2007) The formation, structure, and ageing of As-rich hydrous ferric oxide at the abandoned Sb deposit Pezinok (Slovakia). Geochim Cosmochim Acta 71:4206–4220

Moravanský D, Lipka J (2004) Phyllosilicates and carbonates from hydrothermally altered metamorphic rocks in the Pezinok Sb-Au deposit, Western Carpathians, Slovakia. Miner Slovaca 36:247–264

Morin G, Calas G (2006) Arsenic in soils, mine tailings, and former industrial sites. Elements 2:97–101

Nickson RT, McArthur J, Ravenscroft P, Burgess WG, Ahmed KM (2000) Mechanism of arsenic release to groundwater, Bangladesh and West Bengal. Appl Geochem 15:403–413

Nordstrom DK (2002) Worldwide occurrences of arsenic in ground water. Science 296:2143–2145

Nordstrom DK, Alpers CN (1999) Negative pH, efflorescent mineralogy, and consequences for environmental restoration at the Iron Mountains superfund site, California. Natl Acad Sci 96:3462–4355

Parkhurst DL, Appelo CAJ (1999) PHREEQC-2, a hydrogeochemical computer program. U.S. Geological Survey Water Resources Investigation Report 99-4259

Rapant S, Vrana K, Bodiš D (1996) Geochemical atlas of Slovakia, I. part: ground water (in Slovak). Ministry of Environment of the Slovak Republic, Bratislava

Romero L, Alonso H, Campano P, Fanfani L, Cidu R, Dadea C, Keegan T, Thornton I, Farago M (2003) Arsenic enrichment in waters and sediments of the Rio Loa (Second Region, Chile). Appl Geochem 18:1399–1416

Romero FM, Armienta MA, Carillo-Chavez A (2004) Arsenic sorption by carbonate-rich aquifer material, a control on arsenic mobility at Zimapán, México, Arch. Environ Toxicol 47(1):1–13

Salzsauler KA, Sidenko NV, Sherriff BL (2005) Arsenic mobility in alteration products of sulphide-rich, arsenopyrite-bearing mine wastes, Snow Lake, Manitoba, Canada. Appl Geochem 20:2303–2314

Schreiber ME, Simo JA, Freiberg PG (2000) Stratigraphic and geochemical controls on naturally occurring arsenic in groundwater, eastern Wisconsin, USA. Hydrogeol J 8:161–176

Smedley PL, Kinniburgh DG (2002) A review of source, behaviour and distribution of arsenic in natural waters. Appl Geoch 17:517–568

Smedley PL, Kinniburgh DG, Macdonald DMJ, Nicolli HB, Barros AJ, Tullio JO, Pearce JM, Alonso (2005) Arsenic association in sediments from the loess aquifer of La Pampa, Argentina. Appl Geochem 20:989–1016

Sracek O, Bhattacharya P, Jacks G, Gustafsson JP, von Brömssen M (2004) Behavior of arsenic and geochemical modeling of arsenic enrichment in aqueous environments. Appl Geochem 19:169–180

Sracek O, Armienta MA, Rodriguez R, Villasenor G (2010) Discrimination between diffuse and point sources of arsenic in Zimapan, Hidalgo state, Mexico. J Environ Monitor 12(1):329–337

Stollenwerk KG (2003) Geochemical processes controlling transport of arsenic in groundwater: a review of adsorption. In: Welch AH, Stollenwerk KG (eds) Arsenic in ground water: geochemistry and occurrence. Kluwer, Dordrecht, pp 67–100

Trtikova S (1999) Iron ochres—products of weathering process at Fe and Sb-Au-As ore deposits of Male Karpaty (in Slovak). Dissertation, Comenius University in Bratislava

Trtikova S, Chovan M, Kusnierova M (1997) Oxidation of pyrite and arsenopyrite in the mining wastes (Pezinok-Malé Karpaty Mts.). Folia Fac Sci Nat Univ Mas Brun Geol 39:159–167

Vink BW (1996) Stability relations of antimony and arsenic compounds in the light of revised and extended Eh-pH diagrams. Chem Geol 130:12–30

Walker FP, Schreiber ME, Rimstidt JD (2006) Kinetics of arsenopyrite oxidative dissolution by oxygen. Geochim Cosmochim Acta 70:1668–1676

Whiting KS (1992) The thermodynamics and geochemistry of as with the application to subsurface waters at the Sharon steel superfund site midvale, Utah. MSc thesis, Colorado School of Mines

Williams M (2001) Arsenic in mine waters: an international study. Environ Geol 40:267–278

Wilson SC, Lockwood PV, Ashley PM, Tighe M (2010) The chemistry and behaviour of antimony in the soil environment with comparison to arsenic: a critical review. Environ Pollut 158:1169–1181

Yunmei Y, Yongsuan Z, Williams-Jones AF, Zhenmin G, Dexian L (2004) A kinetic study of the oxidation of arsenopyrite in acidic solutions: implications for the environment. Appl Geochim 19:435–444